Analysis of Temperature Coefficients of Bifacial Crystalline Silicon PV Modules

Juan Lopez-Garcia, Diego Pavanello, and Tony Sample

***Abstract*—Bifacial c-Si photovoltaic (PV) modules can increase the performance of traditional PV modules because both sides of the cells, front and rear, absorb solar radiation. The knowledge of the temperature coefficients (TCs) is relevant to compare indoor and on-field performance of PV devices. In this paper, the TCs of c-Si bifacial PV modules from five different manufacturers were measured under natural sunlight and simulated indoor condition with a large-area steady-state solar simulator and the data were compared with the datasheet values. The effects on the TCs of an opaque and a reflective rear cover were also analyzed. There were no relevant differences between indoor and outdoor and for front and rear side TCs (within the measurement uncertainty). Slight differences with respect to the datasheet values were found for most of the modules under test for the TC for current α and for maximum power δ coefficients. However, since the manufacturers do not declare the TC uncertainty, a definitive statement cannot be made.**

***Index Terms*—Bifacial, photovoltaic (PV), temperature coefficient (TC).**

I. Introduction

THE dependency of the performance of photovoltaic (PV) modules on temperature is well known [1]–[6] and the procedures for temperature and irradiance corrections of current–voltage characteristics taken in the field to standard test conditions (STC) are described in the International Standard IEC 60891 [7]. In the equations appear the three temperature coefficients (TCs): short-circuit current TC, α, open-circuit voltage TC, β, and maximum power TC, δ. The TCs measurements are required for accurate yield estimates and modules energy rating and the manufacturers include these parameters in the datasheet. Bifacial c-Si PV modules can increase the performance of traditional PV modules because both sides of the cells, front and rear, absorb solar radiation. To assess their performance and quality, PV modules are measured and characterized in a controlled environment under STC as defined by the International Electrotechnical Commission (IEC) [8]. However, although the IEC is working on the development of a draft technical specification for bifacial PV devices IEC TS 60904-1-2 [9], there is currently no standard for bifacial modules. The lack of standards for bifacial c-Si PV modules leads each manufacturer to claim different amounts for the "added value" of the bifaciality which makes it difficult for customers to directly compare between bifacial manufacturers. Furthermore, the manufacturers datasheet only mention the TC under STC conditions and it is assumed that it is for the front side since there is no definition of STC conditions for the rear side. The knowledge of the TCs for the front and rear side of a bifacial module is important in order to compare indoor and on-field performance of PV devices and increase the acceptance by the customers. Although curves measured under indoor environment in most cases do not need TCs for an accurate correction (because laboratory conditions of irradiance and temperature are close to target conditions), this is not often the case for outdoor measurements.

It is known that the higher the $V_{\rm oc}$ of a solar cell, the smaller the temperature dependency of the $V_{\rm oc}$ and hence the $P_{\rm max}$ [6]. It was also reported in the 1990s that the bifacial solar cell technologies such as passivated emitter rear cell (PERC) increased the $V_{\rm oc}$ and then they presented a lower temperature dependency of their $V_{\rm oc}$ [3]. Furthermore, due to the fact that the monofacial cells have a full-area rear metal contact and the bifacial cell presents a largely "open" rear surface, bifacial cells absorb less infrared (IR) light and hence operate at lower temperatures compared to monofacial cells [5]. However, a relative high IR absorption was also observed in PERC cells due to free carrier absorption in the n+−diffused emitters of the cells in connection with the light trapping effects due to the front surface texture. In addition, owing to the high bulk series resistance, the temperature dependence of their fill factors increased. New bifacial solar cell structures (n and p-type) appeared (passivated emitter, rear locally-diffused (PERL), passivated emitter rear totally diffused (PERT), (n-PERT), heterojunction with intrinsic thin-layer (HIT)) with improved minority carrier lifetime and also with high $V_{\rm oc}$ decreasing the temperature dependency of the electrical parameters [3]. The question that arises is whether a single set of equations (used for traditional monofacial modules) can also apply for bifacial modules, using the same parameters for both faces. The hypothesis to be tested is whether the measurement method, set up, and conditions have to be different for bifacial modules and how these set up and measurement conditions agreed with the IEC draft technical specification indications. The paper is focused on the experimental assessment of the particular measurement methods that may or may not be

Manuscript received March 19, 2018; revised May 3, 2018; accepted May 6, 2018. Date of publication May 24, 2018; date of current version June 19, 2018. This work was supported by the EMPIR programme cofinanced by the Participating States and from the European Union's Horizon 2020 research and innovation programme. *(Corresponding author: Juan Lopez-Garcia.)*

The authors are with the European Commission, Joint Research Centre, Energy, Transport and Climate, Energy efficiency and Renewables Unit, European Solar Test Installation, Ispra 21027, Italy (e-mail: juan.lopez-garcia@ec.europa.eu; diego.pavanello@ec.europa.eu; tony.sample@ec.europa.eu).

Color versions of one or more of the figures in this paper are available online at http://ieeexplore.ieee.org.

Digital Object Identifier 10.1109/JPHOTOV.2018.2834625

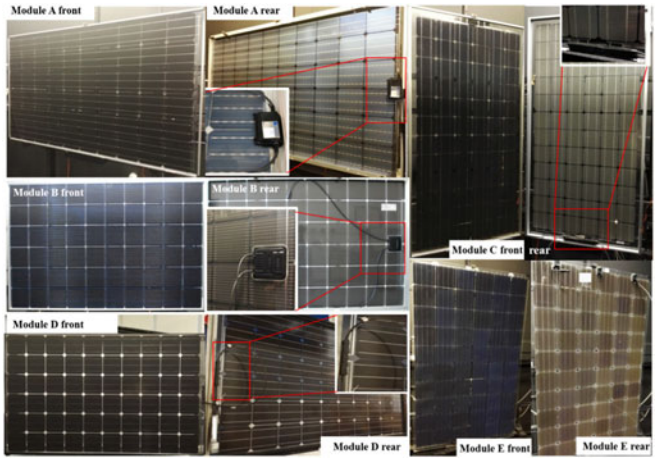

Fig. 1. Front side and rear side images of the c-Si bifacial modules under test. A zoom of the junction box area is included.

applied to bifacial PV modules instead of standard monofacial PV modules.

The aim of this paper is to analyze and compare the TC for α, β, and δ of both sides of bifacial c-Si PV modules measured under natural sunlight and simulated indoor conditions and to compare with the rated values obtained from the manufacturer's datasheet and nameplate. To our knowledge, there are no previous experimental studies reported in the literature on TCs on c-Si bifacial PV modules.

II. Experimental Details

A. Devices Measured

Different commercially available bifacial n-type crystalline Si (four glass/glass and one glass/foil) modules (both framed and frameless) from five manufacturers were characterized under simulated (indoor) and natural sunlight in the outdoor test field at the European Solar Test Installation (ESTI) under STC conditions. The modules consisted of 60 or 72 cells in three substrings and they were light-soaked before the measurements to eliminate possible light induced degradation following the standard IEC 61215-2 [10]. Fig. 1 shows the front and rear images of the bifacial modules under test. The front and rear side of the module has been defined by the manufacturer, in practice it means that the rear side is that side incorporating the junction box or labels. Modules D and E are frameless (PERC and n-PERT cell technologies, respectively) while modules A, B, and C are framed (PERC, n-PERT, and HIT cell technologies, respectively).

It should be noted that modules A and B have a lip of the frame covering a small part of the rear of the cells, whereas module C has wider edge spacing avoiding any shade to the rear cell surface. Modules A, B, and E have junction boxes partially covering the rear side cells. In the case of module E, the three junction boxes are covering cells in each of the three substrings.

B. I–V Measurement Setup

I–V curves of the bifacial modules were measured indoor with a class AAA large-area steady-state solar simulator (2×2 m^2) with a sweep time $\sim$1 s. On exposure to constantartificial illumination of $\sim$1000 W/ m^2, the module temperature increased with exposure time. Periodic *I–V* curves were taken over a range of temperature spanning at least 30 °C, as mentioned in the IEC 60891 [7]. The temperature rise of each module was monitored by means of five temperature sensors attached to the rear surface of the module. The reference cell was mounted coplanar to the module and its temperature controlled by a Peltier element. It has been reported that the indoor testing of high capacitive bifacial PV modules with a standard flash solar simulator (sweep time $<$100 ms) may be affected by strong measurement artefacts and lead, depending on the pulse duration and sweep speed, to underestimations of the measured power [11]. In this case, the steady-state solar simulator leads to more accurate measurements of *I–V* curves for bifacial PV modules than the standard pulsed solar simulators with a forward sweep single flash.

For the outdoor measurement setup, the modules were mounted on a solar tracker (normal global sunlight) and heated by natural sunlight under clear sky conditions. Before the measurements, the module was cooled to temperatures below ambient temperature in the shade by running tap water.

The electrical characterization of the modules (both indoor and outdoor) was carried out according to the draft technical specification IEC TS 60904-1-2 for single-side illumination of bifacial modules with a rear cover, with the same dimensions as the module, placed in direct contact with the nonilluminated surface of the module. The contribution from the light incident on the opposite side of the device under test must be eliminated during the measurement by creating a nonirradiated background (rear irradiance should not exceed 3 W/ m^2, at any point, on the nonexposed side of the device). A black ("nonreflective") painted wooden panel according to the IEC TS 60904-1-2 with an average optical reflectance of 4% was used. In addition, a gloss white sheet reflective panel was also used as opposition to the opaque panel with an optical reflectance above 93% in the range 350–1200 nm. The optical reflectance at room temperature of the rear wooden panels was measured with a Perkin–Elmer LAMBDA 9 spectrophotometer. *I–V* curves were obtained by illuminating alternatively the front or the rear side. *I–V* curves (both indoor and outdoor) were corrected to STC (1000 W/m2, 25 °C and AM1.5).

The spectral responsivity of the modules were measured using a differential spectral responsivity technique with a large area pulsed solar simulator equipped with a number of bandpass filters to obtain illumination of modules with quasi-monochromatic light [12].

III. Results and Discussion

A. Temperature Distribution

In order to study the temperature gradient in the bifacial modules, five temperature sensors (PT100) were symmetrically placed in the rear side or nonilluminated surface of the module (see Fig. 2), just behind a cell, in the corners and in the middle (position 3) during the current–voltage measurement in the continuous light solar simulator with the same irradiance conditions. Figs. 3 and 4 show the temperature as a function of the time for framed and frameless bifacial modules, respectively.

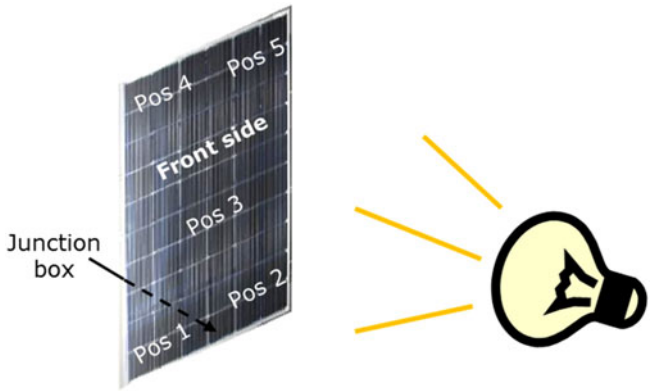

Fig. 2. Schematic representation of the temperature sensors positions for the temperature control.

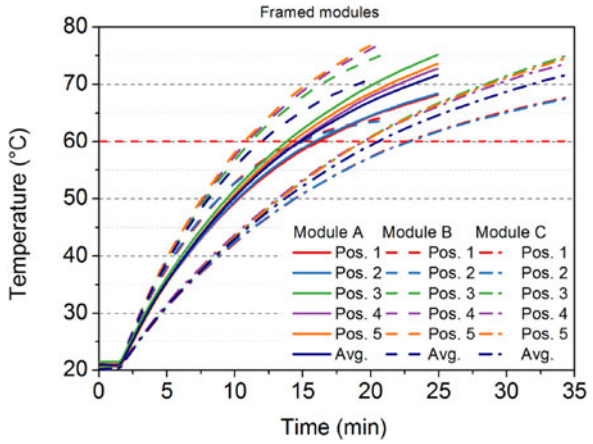

Fig. 3. Comparison of temperature measured in five different positions and the average module temperature of framed bifacial modules as a function of time.

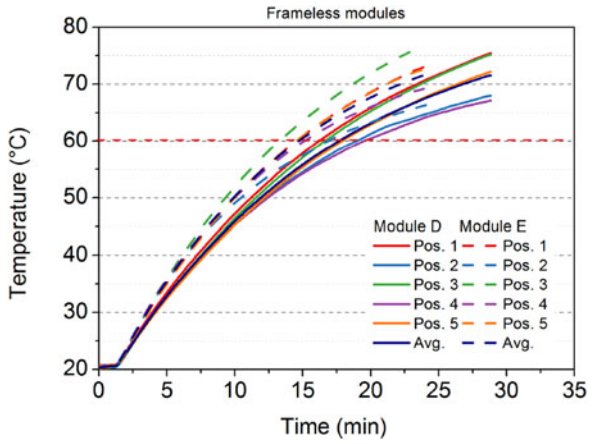

Fig. 4. Comparison of the temperature measured in five different positions and the average module temperature of frameless bifacial modules as a function of time.

Differences up to 10 °C were observed between the middle and the edges of the modules in the continuous light simulator probably due to the heating of the air in the top side of the modules. Module B, glass/transparent foil, required less time to increase the temperature than the more massive glass/glass

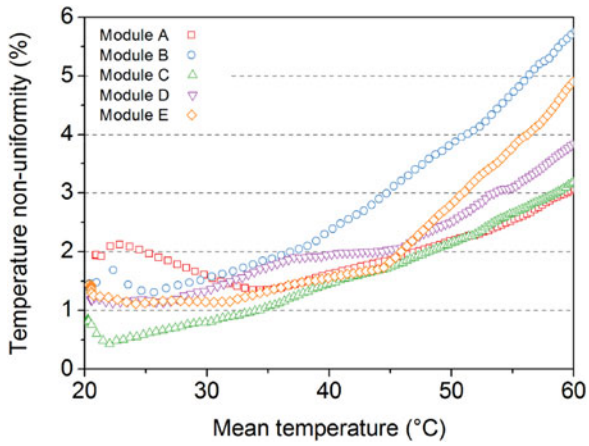

Fig. 5. Temperature nonuniformity as a function of the mean temperature of five sensors for bifacial modules.

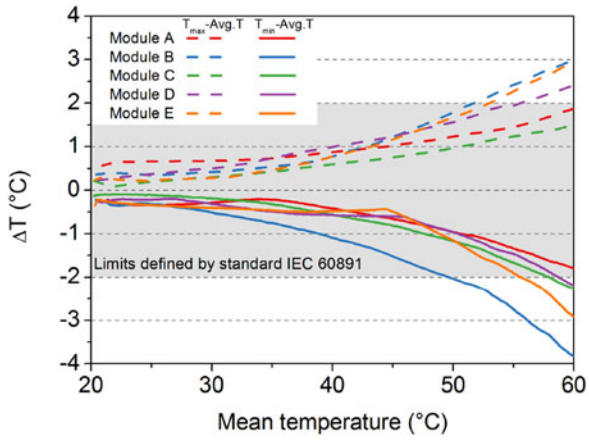

Fig. 6. Temperature variation from the average as a function of the mean temperature of five sensors for bifacial modules. The limits for temperature deviation from the average are shown in grey.

modules as has been reported previously [2]. However, module B exhibited the largest temperature gradient across the module. Frameless modules reached 60 °C from the ambient temperature condition in a time between 15 and 18 min. Module C, with 72 cells, reached 60 °C in around 20 min.

The nonuniformity of the temperature is defined as follows:

$$\text{Nonuniformity}\,(\%) = \frac{T_{\max} - T_{\min}}{T_{\max} + T_{\min}} \times 100 \qquad (1)$$

where $T_{\max}$ and $T_{\min}$ are the maximum and minimum temperatures in °C, respectively, of the five sensors at a certain moment. According to the standard IEC 60891 for procedures for temperature and irradiance corrections to measured *I–V* characteristics, the temperature of the module should be measured in at least four points and their values averaged. It is also mentioned that the temperature should be uniform within ±2 °C from the average value.

Figs. 5 and 6 show the temperature nonuniformity and the temperature variation from the average of five points for the framed and frameless modules under test, respectively, as a function of the mean temperature of the five sensors. The

temperature variation has been defined as follows:

$$\Delta T\,(^{\circ}\mathrm{C}) = T_{\max} - T_{\text{average}} \tag{2}$$

$$\Delta T\,(^{\circ}\mathrm{C}) = T_{\min} - T_{\text{average}} \tag{3}$$

where $T_{\max}$ (°C), $T_{\min}$ (°C), and T_{average} are the maximum, minimum, and average temperatures, respectively, of the five sensors at a certain moment. *I–V* curves and the TCs were measured for temperatures below 60 °C (both indoor and outdoor). In general, the temperatures of the modules were within the temperature uniform limits of ±2 °C for the range of interest with the exception of the single module B. A slightly greater deviation from the average at temperatures above 55 °C was found for frameless modules D and E. The temperature nonuniformity increased with the mean temperature up to values around 5%–6% for modules E and B, respectively. The nonuniformity was among 1%–2% up to temperatures around 46 °C, where the slope changed. This result is in good agreement with the temperature analysis performed under real outdoor condition for similar modules [13], where it was reported that the average temperature and the nonuniformity depends on the number and position of the temperature sensors and can lead to an under or overestimation of the temperature. The TCs were calculated from the temperature sensor placed in the position closer to the average value.

When temperature sensors, such as PT100, are used to determine the cell temperature of PV devices under natural or simulated steady-state irradiance, two main problems arise. First, a considerable spread of temperature can be observed over the area of the module. Second, as the solar cells are usually not accessible, sensors are attached to the back of the module and the measured temperature thus is influenced by the thermal conductivity of the encapsulant and back materials. These problems are aggravated when determining the equivalent cell temperature (ECT) for on-site measurements of array performance where all cells have slightly different temperatures and one cannot easily determine the average cell temperature. The ECT is the average temperature at the electronic junctions of the device which equates to the current operating temperature if the entire device were operating uniformly at this junction temperature. The ECT can be calculated by means of the open-circuit voltage method described in the IEC 60904-5 [14] if the TC and the open-circuit voltage at STC conditions are known by mean of the equation

$$\mathrm{ECT} = T = T_{\mathrm{STC}} + \frac{1}{\beta}\left[\frac{V_{\mathrm{oc}}}{V_{\mathrm{oc,\ STC}}} - 1 - a\ln\left(\frac{G}{G_{\mathrm{STC}}}\right)\right] \tag{4}$$

where T is the temperature (°C) of the module, V_{oc} the open-circuit voltage at temperature T, β is the TC for the open-circuit voltage (1/°C), T_{STC} is 25 °C, $V_{\mathrm{oc,STC}}$ is the open-circuit voltage at STC conditions, G_{STC} is 1000 W/ m^2, G is the irradiance at temperature and voltage T and V_{oc}, and a is a parameter that depends on the voltage and irradiance. For indoor conditions with the type of solar simulator used, the incident irradiance $G \sim G_{\mathrm{STC}}$, and (4) can be simplified. Fig. 7 shows the variation between the ECT and the measured temperature during the *I–V* curve acquisition. Positive values of ΔT = (ECT– T) indicate an underestimation of the module temperature during the *I–V* curve measurement and negative values imply an overestimation. Modules A, B, and D showed a slight temperature underestimation below the standard limit of +2 °C. Modules C and E exhibited a slightly overestimation of the module temperature between 0 and –1 °C. This indicates that the standard requirement for temperature stability can be fulfilled for indoor measurement and the TCs calculated are reliable.

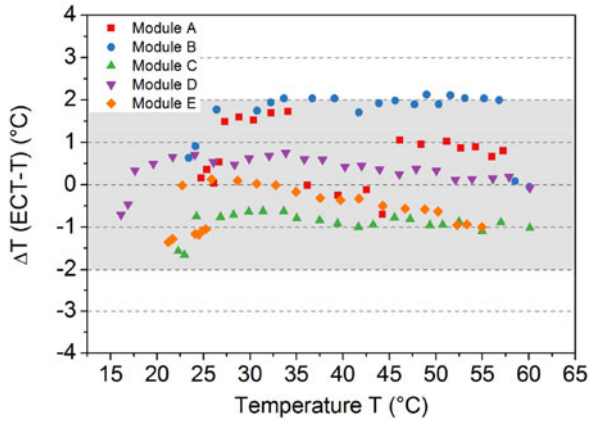

Fig. 7. Difference between the equivalent cell temperature (ECT) and the measured temperature as a function of the temperature.

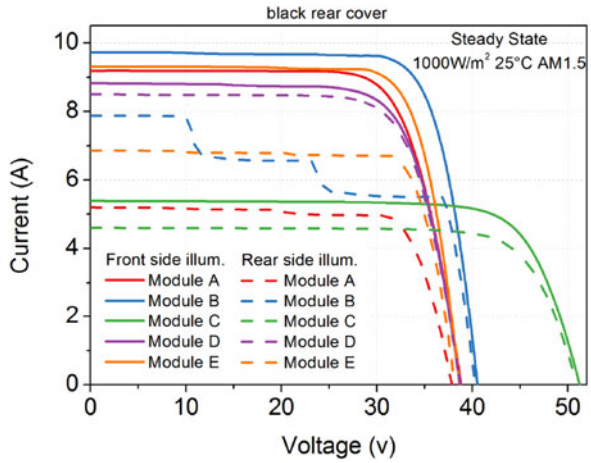

Fig. 8. *I–V* curves of commercially available Si bifacial modules measured indoor with a steady-state solar simulator under STC conditions with a black rear cover.

B. Measurement of Electrical Parameters

Fig. 8 shows the *I–V* curves at STC conditions of framed and frameless modules from different manufacturers, namely from A to D, measured indoor with a steady-state solar simulator with a nonreflective black rear cover. Both front and rear illuminations were tested. It should be noted that the design of the module, in particular, the junction box location and frame "self-shading" have a strong influence on the *I–V* curves of the rear side. Partial shading of the rear cells due to covering by the lips of the frame or junction boxes lead to nonuniform rear irradiance and kinks in the rear *I–V* curves.

Modules A, B, and E show up to three marked kinks in the *I–V* curves of the rear side due to the partial shading of the cells by the junction box (all three cases) and the frame (modules A

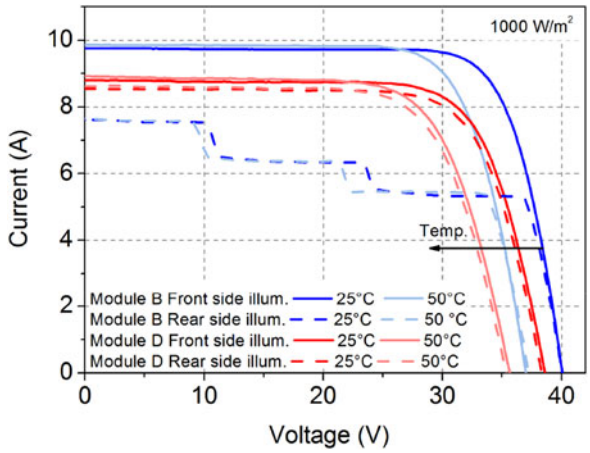

Fig. 9. *I–V* curves of module B and D front side and rear side at 25 °C and 50 °C measured indoor with a steady-state solar simulator.

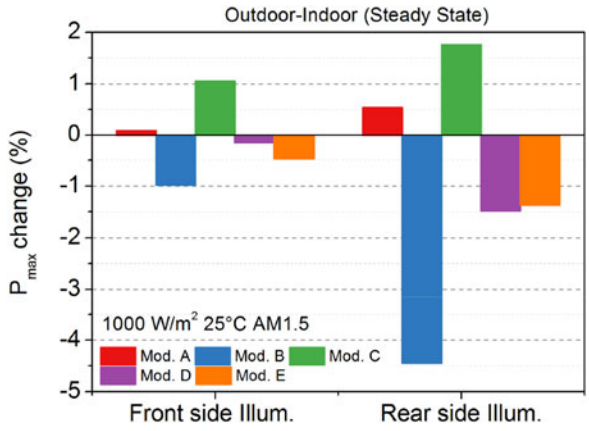

Fig. 10. $P_{\max}$ difference between the outdoor and indoor measurements at STC for front and rear side illumination using an opaque rear cover.

and B). It is especially relevant with the case of the module B with a big junction box covering almost half of two cells of a substring and the lips of the frame covering partially the cells at the edge of the module which reduce the rear I_{mpp} and $P_{\max}$.

According to the draft technical specification for bifacial PV modules, IEC TS 60904–1–2 [9], from the measured front and rear I-V curves, the maximum power bifaciality $\varphi_{P\max}$ of the modules under test can be calculated and a wide range of values were obtained: 58%, 66%, 86%, 97%, 76%, for modules A–E, respectively.

If we continue obtaining *I–V* curves as the module is heating up by the radiation, the voltages are shifted toward lower values while the short-circuit current slightly increases as is shown in Fig. 9. *I–V* curves of the front side and rear side of the representative framed and frameless modules (B and D) for 25 and 50 °C are plotted in Fig. 9. Under STC conditions, the difference between the $P_{\max}$ measured indoor and under natural sunlight or outdoor, $P_{\max}$ change, can be defined as follows:

$$P_{\max}\text{change}\,(\%) = \frac{P_{\max\,\text{outdoor}} - P_{\max\,\text{indoor}}}{P_{\max\,\text{indoor}}} \times 100. \quad (5)$$

A $P_{\max}$ change within $\pm 1\%$ when the front side is illuminated was obtained as shown in Fig. 10 according to the draft technical specification IEC TS 60904–1–2 for single-single side illumination method. For the rear side, there are slightly greater differences with the outlier of module B. The best declared ESTI $P_{\max}$ uncertainty for a large-area steady-state solar simulator and outdoor measurement, $\pm 1.7\%$, is well below the $P_{\max}$ change uncertainty. This means that for STC front conditions, the outdoor and indoor measurement systems are consistent.

C. Temperature Coefficients: Indoor and Outdoor Measurements

Fig. 11(a)–(c) shows the short-circuit current, open-circuit voltage, and maximum output power as a function of the average module temperature for modules A, B, and C indoor measured with a continuous solar simulator. The figures also show the electrical parameter for the front and rear side of the module. Short-circuit current exhibits a slightly linear increasing trend for both side of the bifacial module. In contrast, the open-circuit voltage and the maximum output power shows a linear decrease with the temperature. The TCs for current, α, for voltage, β, and for power, δ, can be calculated from the slope of the curves. Similar curves, with the same trend, were obtained for measurements under natural sunlight outdoors (not shown here).

The TC α, β, and δ for indoor and outdoor measurements and for the front side and rear side of the modules are shown in Fig. 12(a)–(c), respectively, together with the value of the TC given by the manufacturer in the datasheet. In general, a slight difference of the TC for current, α, for front and rear both indoor and outdoor has been found. This deviation is within the measurement uncertainties with two exceptions for the rear side measured under natural sunlight, modules B and D. The zero or near zero value for the rear side illumination in outdoor condition for modules B and E should be noted. The error bars represent the expanded uncertainty (U95% $k = 2$) of the measurements. The determination of the TC uncertainties for bifacial modules uses the c-Si modules uncertainties declared by ESTI as an accredited laboratory by the Italian National Accreditation Body and the complete development is explained in internal quality system procedures and internal reports of the European Commission. In general, the uncertainty contribution includes parameter related to the electrical uncertainty (data acquisition system), temperature uncertainty (indicators, measurement conditions for reference cells, for device under test, nonuniformity in test device), and variation on the spectral mismatch correction factor that include the slight dependency of the spectral response (SR) with the temperature for c-Si modules (it was estimated that the mismatch factor (MMF) varies due to the variation of c-Si SR with temperature, by $\pm 0.05\%$ ($k = 2$) over a 30 °C range under natural sunlight and slightly lower for simulated light) [15], [16]. Fig. 12(a) also shows the rated value from the datasheet. A disagreement beyond the measurement uncertainty between the datasheet and front side indoor and outdoor α measured values was obtained for modules B, C, and D. However, it is difficult to make definitive statements or comparisons since the manufacturers do not declare the un-

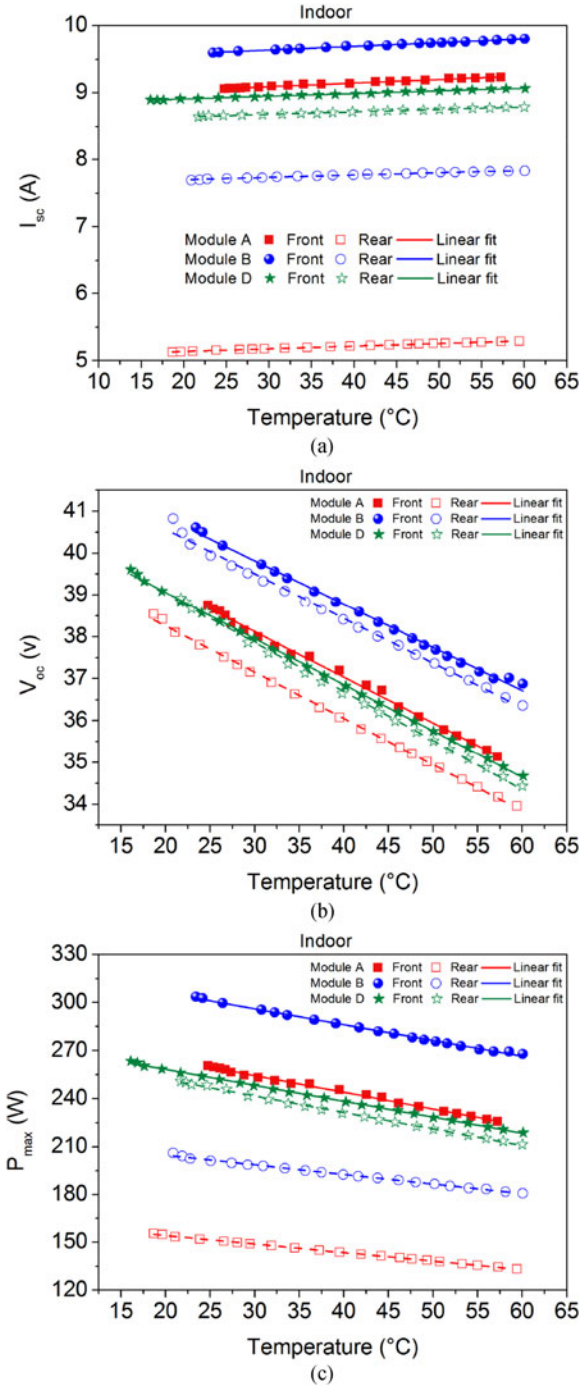

Fig. 11. Plot of (a) short-circuit current, (b) open-circuit voltage, and (c) maximum output power versus module temperature for indoor measurements of three bifacial modules for the front and rear side illumination.

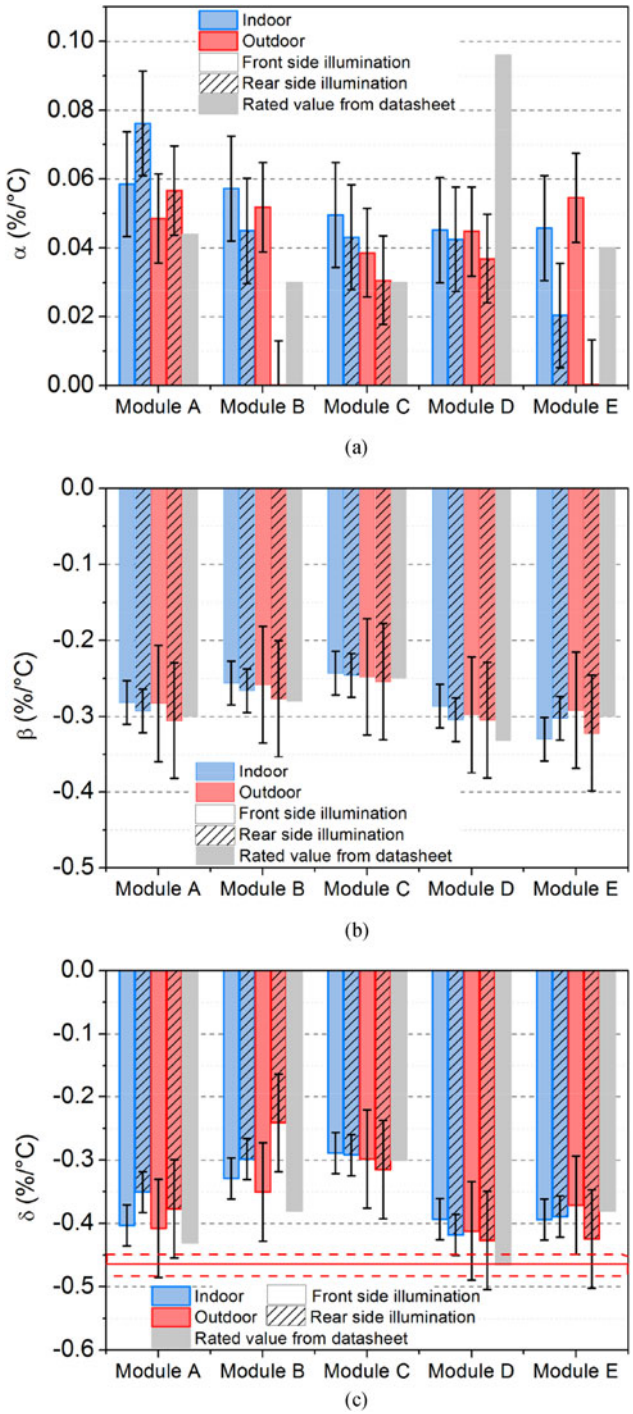

Fig. 12. Temperature coefficient for (a) short-circuit current, α, (b) open-circuit voltage, β, and (c) maximum output power, δ, for the front and rear side of bifacial modules measured on indoor and outdoor conditions. The rated value for the TC from the datasheet is also plotted. The average δ value and standard deviation of c-Si PV monofacial modules tested at ESTI are also plotted in Fig. 12(c) as a red line and dotted line, respectively.

certainties in TC in their datasheets. The TC for voltage, β, is shown in Fig. 12(b) for the front and rear side of the bifacial modules measured under indoor and outdoor conditions. Similar coefficients were obtained for the front and rear side of the modules. No significant differences were observed for the TC for voltage between the indoor and outdoor measurements. Furthermore, β was in good agreement with the values given by the manufacturers.

Fig. 12(c) exhibits the TCs for power, δ, for the front and rear side of bifacial modules measured under simulated (indoor) and natural sunlight (outdoor). The modules under test presented similar TC values for the front and rear side for both indoor and outdoor methods within the measurement uncertainties. The differences below 1% between the steady state and

TABLE I
PERCENT DIFFERENCE $D_{\%}$ AND PERFORMANCE STATISTIC SCORES, e_n, BETWEEN OUTDOOR AND INDOOR MEASUREMENTS FOR THE FRONT AND REAR SIDE

Module	FRONT SIDE						REAR SIDE					
	α		β		δ		α		β		δ	
	$D_{\%}$	E_n	$D_{\%}$	E_n	$D_{\%}$	E_n	$D_{\%}$	E_n	$D_{\%}$	E_n	$D_{\%}$	E_n
A	-17.1	0.5	0.5	0.0	1.1	0.1	-25.7	1.0	4.4	0.2	7.5	0.3
B	-9.4	0.3	0.8	0.0	6.6	0.3	-99.8	2.3	4.0	0.1	-19.2	0.7
C	-22.2	0.6	2.0	0.1	3.1	0.1	-29.0	0.6	3.4	0.1	7.8	0.3
D	-0.9	0.0	4.0	0.1	4.8	0.2	-13.2	0.3	0.3	0.0	2.2	0.1
E	19.1	0.4	-11.5	0.5	-13.5	0.7	-98.2	1.0	6.6	0.2	9.1	0.4

the outdoor system for STC conditions are also conserved for other temperatures that imply a small variation in the TC for power.

A slight divergence between ESTI measured δ values and the manufacturer datasheet values are observed. However, as in the case for the TC for current and voltage, manufacturers do not declare their uncertainties. It is also observed that the TC of the module C (HIT technology) is markedly lower (up to 25% lower in some cases) than the others (PERC and PERT). In spite of that, the bifacial modules are Si-based technologies; it seems that the TCs of bifacial modules are more dependent on the cell technology rather than on the measurement method or the module side. The TCs for power data have been compared with a set of 33 poly and mono c-Si PV monofacial modules tested at ESTI in the last years. The average δ value and the standard deviation (–0.463 $\pm$ 0.016%/°C) are plotted in Fig. 12(c) and resulted to be greater than the measured values for bifacial PV modules.

In this paper, the percent difference $(D_{\%})$ and the performance statistic score, E_n numbers, are reported for different values according to the international standard ISO/IEC 17043 that describe the common performance statistics [17]. Percent difference was calculated as follows:

$$D_{\%} = \frac{A - B}{B} \times 100 \tag{6}$$

where *A* is the measurement result of a given system (TCs in a certain situation, i.e., outdoor, white cover, rear illumination, etc.), and *B* is the reference value. Having consistent uncertainty estimation for all measurement systems allowed for the calculation of the E_n numbers that can be used to validate the uncertainty estimation. The E_n number is defined as follows:

$$E_n = \frac{A - B}{\sqrt{(U_A)^2 + (U_B)^2}} \tag{7}$$

where U_A is the expanded uncertainty associated to the quantity *A*, i.e., at $k = 2$, and U_B is the expanded uncertainty of the reference value *B*, i.e., at $k = 2$. According to ISO/IEC 17043, $|E_n|d1$ are considered "satisfactory" values and $|E_n| > 1$ are considered "unsatisfactory" values, indicating that a further investigation is required. Table I shows the percent differences and E_n numbers for the TCs of the bifacial modules measured outdoor and indoor (reference). A good agreement between the indoor and outdoor TC values with E_n values below 1 with the main differences in the TC for current is observed. Table II shows the percent difference $D_{\%}$ between the front measured values and the rated TCs for indoor and outdoor systems assuming the measured TC as the reference one. The disagreement in β for the module D between our result and the manufacturer is clearly observed. However, the TC for current of the other modules under test is underestimated. In general, the TC for power is also overestimated with differences among 3.7%–18% for indoor and 0.6%–13% for outdoor.

TABLE II
PERCENT DIFFERENCE $D_{\%}$ BETWEEN FRONT MEASURED AND RATED TEMPERATURE COEFFICIENTS FOR INDOOR AND OUTDOOR MEASUREMENTS

Module	INDOOR			OUTDOOR		
	α	β	δ	α	β	δ
A	-24.8	6.5	6.7	-9.3	6.0	5.5
B	-47.6	9.3	15.5	-42.1	8.4	8.4
C	-39.5	2.7	3.7	-22.2	0.6	0.6
D	112.4	15.9	18.3	114.3	11.4	12.9
E	-12.7	-9.0	-11.5	-26.7	2.8	2.3

D. Effects of a Black and White Rear Cover in the Temperature Coefficients

It has been reported that the $I_{\rm sc}$ and $P_{\rm max}$ of bifacial c-Si PV modules can increase up to 4% with a reflective white cover placed at 0 cm from the rear or nonilluminated surface of the module [18], [19]. However, the influence of a reflective white rear cover has been found to be, in general, not so relevant for the TCs and no significant differences between opaque or reflective rear cover have been observed. As shown in Fig. 13, differences below –5% between the black and white covers (that implies a higher $P_{\rm max}$ for the white reflective cover) were found for δ tested under simulated sunlight in indoor conditions. The module E was the only module under test that exhibited slightly greater variations for front and rear side but within the measurement uncertainties. Fig. 14 shows slightly greater differences in δ (in the range of $\pm$7%) between the black and the white cover for modules measured under natural sunlight with deviation within the measurement uncertainty. This means that the set-up conditions for the TC determination of bifacial PV modules can be relaxed and are more flexible

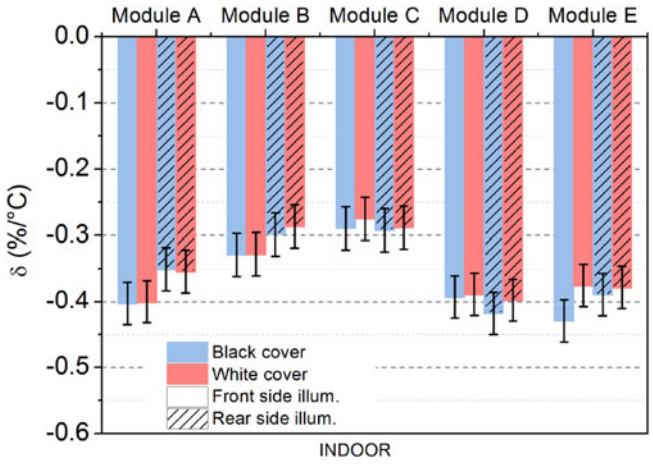

Fig. 13. Temperature coefficient for maximum output power, δ, for the front and rear side of bifacial modules measured on indoor conditions with a black and a reflective white cover.

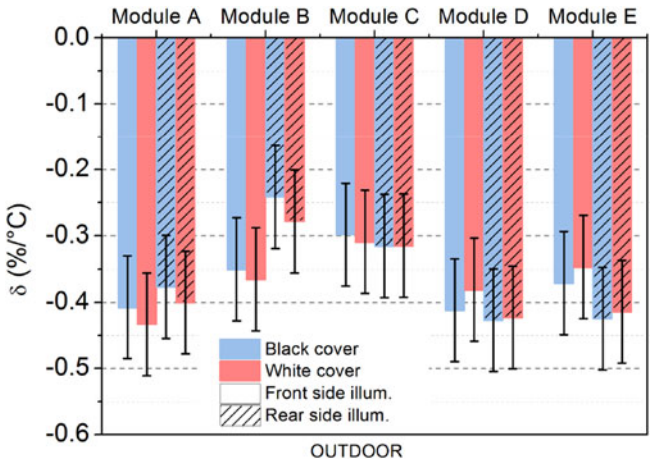

Fig. 14. Temperature coefficient for maximum output power, δ, for the front and rear side of bifacial modules measured under natural sunlight in outdoor conditions with a black and a reflective white cover.

with respect to those *I–V* curve measurements for the electrical characterization.

IV. Conclusion

Crystalline silicon bifacial PV modules from five different manufacturers were characterized indoors and outdoors by means of a steady-state solar simulator and under natural sunlight at the ESTI laboratory and the TCs were measured for the front and rear side of the modules.

With respect to the I–V measurements:

The design of the bifacial module, in particular the junction box, nameplate, and frame location on the rear side plays an important role in the rear performance of the module. *I–V* curves of the rear side partially "self-shaded" led to kinks in the *I–V* curves reducing rear I_{mpp} and $P_{\max}$. Furthermore, in agreement with the draft of the IEC TS 60904–1–2, the parasitic reflections from the rear side of the device under test can increase the $P_{\max}$ and subsequently the uncertainty in measurements. Therefore, the definition of measurement conditions as the rear cover used is recommended in order to obtain reproducible and reliable performance parameters.

With respect to TCs:

There are no significant differences between the TC of the front and rear side for a particular bifacial technology or design. The indoor and outdoor methods yield approximately equal TC and the slight differences are related to the uncertainty associated. The measured TC at ESTI and the values given by the manufacturer in the datasheet were similar for β and δ. However, the manufacturers do not declare the TC uncertainties leading to a difficult comparison with the measured values. Even if indicated in IEC TS 60904–1–2 draft for *I–V* measurements, opaque rear cover seems to be not so relevant for the TC determination and the TC are more dependent on cell technology rather than on measurement conditions. PV bifacial modules have shown a lower power TC than standard monofacial c-Si modules tested at the ESTI lab which can improve power output.

Acknowledgment

The authors would like to thank D. Shaw and A. Casado for the help in the outdoor measurements.

References

[1] R. Dubey *et al.*, "Measurement of temperature coefficient of photovoltaic modules in field and comparison with laboratory measurements," in *Proc. 42nd IEEE Photovolt. Spec. Conf.*, 2015, pp. 1–5.

[2] D. L. King, J. A. Kratochvil, and W. E. Boyson, "Temperature coefficients for PV modules and arrays: Measurement methods, difficulties, and results," in *Proc. 26th IEEE Photovolt. Spec. Conf.*, 1997, pp. 1183–1186.

[3] J. Zhao, A. Wang, S. J. Robinson, and M. A. Green, "Reduced temperature coefficients for recent high-performance silicon solar cells," *Prog. Photovolt. Res. Appl.*, vol. 2, pp. 221–225, 1994.

[4] M. A. Green, *Solar Cells- Operating Principles, Technology and System Applications.* Englewood Cliffs, NJ, USA: Prentice-Hall, 1982.

[5] A. Huebner, A. G. Aberle, and R. Hezel, "Temperature behavior of monofacial and bifacial silicon solar cells," in *Proc. 26th IEEE Photovolt. Spec. Conf.*, Piscataway, NJ, USA, 1997, pp. 223–226.

[6] J. C. C. Fan, "Theoretical temperature dependence of solar cell parameters," *Sol. Cells*, vol. 17, pp. 309–315, 1986.

[7] *Photovoltaic Devices: Procedures for Temperature and Irradiance Corrections to Measured I-V Characteristics*, IEC 60891, 2009.

[8] *Solar Photovoltaic Energy Systems – Terms, Definitions and Symbols*, IEC 61836, 2016.

[9] *Measurement of Current-Voltage Characteristics of Bifacial Photovoltaic (PV) Devices*, IEC TS 60904-1-2, 2017.

[10] *Crystalline Silicon Terrestrial Photovoltaic (PV) Modules: Design Qualification and Type Approval*, IEC 61215-2, 2016.

[11] J. Lopez-Garcia, B. Haile, D. Pavanello, A. Pozza, and T. Sample, "Characterisation of n-type bifacial silicon PV modules," in *Proc. 32nd Eur. Photovolt. Sol. Energy Conf. Exhib.*, Munich, Germany, 2016, pp. 1724–1729.

[12] R. Van Steenwinkel, "Measurements of spectral responsivities of cells and modules," in *Proc. 7th Eur. Photovolt. Sol. Energy Conf. Exhib.*, Sevilla, Spain, 1986, pp. 325–329.

[13] R. Kenny, E. Garcia-Menendez, J. Lopez-Garcia, and B. Haile, "Characterising the operating conditions of bifacial modules," in *Proc. 8th Int. Conf. Crystalline Silicon Photovolt.*, Laussanne, Switzerland, 2018.

[14] Determination of the Equivalent Cell Temperature (ECT) of Photovoltaic (PV) Devices by the Open-Circuit Voltage Method, IEC 60904-5, 2011.

[15] H. Müllejans, W. Zaaiman, and E. D. Dunlop, "Reduction of uncertainties for photovoltaic reference cells," *Metrologia*, vol. 52, pp. 646–653, 2015.

[16] H. Müllejans, W. Zaaiman, and R. Galleano, "Analysis and mitigation of measurement uncertainties in the traceability chain for the calibration of photovoltaic devices," *Meas. Sci. Technol.*, vol. 20, 2009, Art. no. 075101.

[17] Conformity Assessment – General Requirements for Proficiency Testing, ISO/IEC 17043:2010, 2010.
[18] J. P. Singh, S. Guo, I. M. Peters, A. G. Aberle, and T. M. Walsh, "Comparison of glass/glass and glass/backsheet PV modules using bifacial silicon solar cells," *IEEE J. Photovolt.*, vol. 5, no. 3, pp. 783–791, May 2015.
[19] B. B. Van Aken and A. J. Carr, "Relating indoor and outdoor performance of bifacial modules," in *Proc. 40th IEEE Photovolt. Spec. Conf.*, 2014, pp. 1381–1383.

Juan Lopez-Garcia received the bachelor's degree in physics from the Autonomous University of Madrid, Madrid, Spain, in 2006, and the Ph.D. degree in physics focused on material science for photovoltaic applications from the Research Centre for Energy, Environment and Technology (CIEMAT), Madrid, in 2010.

He is a Scientific Officer with the Energy Efficiency and Renewables Unit, Joint Research Centre, European Commission, Ispra, Italy. He also worked with the Catalan Institute of Energy Research in 2012. He specialized on thin-film materials research for photovoltaic applications and research on solar cells and PV modules reliability and degradation.

Diego Pavanello was born in 1980. He received the first degree in music from Conservatory of Piacenza, Piacenza, Italy, in 2001, and the second master's degree in aerospace engineering from Politecnico of Milan, Milan, Italy, in 2005, with a specialization in fluid dynamics.

From 2005 to 2008, he worked with the Joint Research Centre, European Solar Test Installation laboratories, Ispra, Italy, then from 2008 to 2010 with Mecaer Aviation Group in the aerospace sector. He came back to photovoltaics at SUPSI Lugano from 2010 to 2012 and finally he came back to Joint Research Centre as a permanent Research Assistant. His main research interests include measurement uncertainty theory and photovoltaics.

Tony Sample received the bachelor's and Ph.D. degrees in chemistry from Nottingham University, Nottingham, U.K., in 1986 and 1990, respectively.

He is a Scientific Officer with the Energy Efficiency and Renewables Unit, Joint Research Centre, European Commission, Ispra, Italy. Since 1998, he has been working as part of the team with the European Solar Test Installation, Ispra. His research interests include calibration of PV devices and the assessment of lifetime. He is currently the Convenor of the IEC and CENELEC standards working groups on PV modules.